RSC Mechanochemistry

ROYAL SOCIETY OF CHEMISTRY

PAPER

View Article Online
View Journal | View Issue

Cite this: *RSC Mechanochem.*, 2024, **1**, 402

Modeling mechanochemistry: pressure dependence of Diels–Alder cycloaddition reaction kinetics†

Nicholas Hopper,[a] François Sidoroff,[b] Juliette Cayer-Barrioz,[b] Denis Mazuyer,[b] Bo Chen[c] and Wilfred T. Tysoe*[a]

We analyze the effect of pressure on the Diels–Alder (D–A) dimerization reactions using Evans–Polanyi (E–P) theory, a thermodynamic analysis of the way in which a perturbation, in this case a hydrostatic pressure, modifies a reaction rate. Because it is a thermodynamic analysis, the results depend only on the volumes of the initial- and transition-state structures and not on the pathways between them. The volumes are calculated by enclosing the initial- and transition-state structures in a van der Waals' cocoon. Pressure is exerted by multiplying the van der Waals' radii by some factor without allowing the initial- and transition-state structures to relax. The influence of the surrounding solvent is included by using the extreme-pressure, polarizable-continuum method (XP-PCM). The approach is illustrated in detail using cyclopentadiene dimerization for which the rates have been independently measured by two groups. The analysis provides results that are in good agreement with those found experimentally for measurements made up to ~0.3 GPa. The activation volumes of other D–A reactions are calculated in the same way and lead to good agreement for non-polar reactants, but less good agreement for polar ones. The pressure can also distort the initial- and transition-state structures, which can be calculated from the initial- and transition-state Hessians. A pressure-dependent distortion requires knowing the area over which the hydrostatic pressure acts. This is obtained using the Stearn–Eyring postulate that the activation volume is the product of an activation length and the area over which the stress acts. The activation length is obtained from quantum calculations of the difference in the distances between the diene and dienophile in the initial- and transition states. This provides only minor corrections to the results for routinely accessible hydrostatic pressures.

Received 5th June 2024
Accepted 20th July 2024

DOI: 10.1039/d4mr00063c

rsc.li/RSCMechanochem

Introduction

Arguably the most interesting and challenging problems in chemistry, physics and materials science are those that involve stimulating the transformation from one metastable state of the system to another. One method of modifying the rates of such transformations is by exerting forces on the system.[1–11] While mechanochemically induced reactions have been known for millennia,[12] and the grinding of food may have contributed to the development of early hominids,[13] mechanochemistry is perhaps the least well-understood method of modulating chemical reaction rates. Despite this, a large number of mechanochemical reactions have been empirically discovered over the last few years, many of which can be performed with a minimum of solvent and are therefore environmentally friendly, or "green".[1–9,14–22] The large stresses required to induce mechanochemical reactions are often induced at solid–solid interfaces, such as in a ball mill,[23] but it is difficult to study these interfacial processes so that it has been a challenge to rigorously test the validity of mechanochemical models. In addition to being used for chemical syntheses, mechanochemical processes appear to dominate the operation of lubricants[24–26] in perhaps the most economically important subfield of mechanochemistry known as tribochemistry.

The Born–Oppenheimer potential-energy surface (the BO-PES) is at the heart of physicochemical analyses of chemical-reaction rates. Molecules are the stable structures that form at local minima of the PES and calculating reaction kinetics requires measuring the transit rate from one metastable state to another. A challenge is to model the collective behavior of a large number of molecules. This can be accomplished either

[a]Department of Chemistry and Biochemistry, University of Wisconsin-Milwaukee, Milwaukee, WI 53211, USA. E-mail: wtt@uwm.edu
[b]Laboratoire de Tribologie et Dynamique des Systèmes, CNRS UMR5513, Ecole Centrale de Lyon, F-69134 Ecully cedex, France
[c]Donostia International Physics Center, IKERBASQUE, Basque Foundation for Science, 20018 Donostia-San Sebastián, Plaza Euskadi 5, 48009 Bilbao, Spain

† Electronic supplementary information (ESI) available: Computational methods, reaction pathways and structures, a description of the XP-PCM analysis, Fig. S1 to S8, Table S1, description of the curvature analysis, optimized gas-phase geometries and optimized gas-phase structural geometries. See DOI: https://doi.org/10.1039/d4mr00063c

by using the fluctuation-dissipation theorem[27] or by borrowing ideas from statistical thermodynamics by using transition-state theory.[28] Transition-state theory proposes that, while there are an infinite number of possible trajectories from the reactants to the products, the most probable one proceeds *via* the lowest-energy pathway over an activation barrier. The unstable structure at the highest energy of this pathway is known as an "activated complex". It can decompose with equal probabilities to either reform the reactant or form a product. The energy of the activated complex relative to the reactants (the initial state) is the activation energy, and the local PES around this point has one negative force constant (Hessian) due to the structure being unstable. This picture has the advantage of reducing a complex, multidimensional problem to a one-dimensional plot of potential energy as a function of the extent of the reaction, or the "reaction coordinate". The problem is then to calculate the activated complex concentrations using statistical thermodynamics. When transition-state theory was developed, the nature of the activated complex was unclear, although now quantum-mechanical methods have been developed to compute its structure.[29–33] An important consequence of this thermodynamic analysis is that the Gibbs free energy change between the transition- and the initial-states does not depend on the pathways between them. In transition-state theory, the reaction coordinate is merely defined as some value that increases as the reaction proceeds, but has been identified as the path of steepest decent from the transition state to the initial state.[34] One of the most important benefits of transition-state theory is that it provides a formalism that enables chemists to correlate differences in chemical reactivity with molecular structure.[35]

The basic idea that underpins mechanochemistry is that a force or stress modifies the BO-PES to change the energies and locations of the initial- and transition-states of a reaction so as to change the rate constants.[18,20] Judicious modification of the PES can selectively reduce the energy barriers of non-thermally accessible reaction pathways so that they become favorable.[36] The reaction follows the force-displaced stationary points[37] on this modified PES to lead to a so-called Newton trajectory.[38] However, it would be advantageous to develop a theory that maintained the intuitive simplicity of transition-state theory while providing insights into the processes that control mechanochemical reactivity. A perturbation method of transition-state theory has been developed by Evans and Polanyi[39,40] that fulfils these requirements that will be described in greater detail below.

Arguably an impediment to developing and testing theories of mechanochemical reaction rates has been the lack of precise measurements of the kinetics of well-characterized reactions. Fortunately, a large number of hydrostatic-pressure-modified reaction rate have been measured[41–45] to allow mechanochemical theories to be tested.[46–48]

More recently, the rates of mechanochemical reactions have been measured using an atomic-force microscope (AFM) tip compressing or sliding on surfaces.[24,45,49–51] In particular, the ability to characterize the nature of the surface reaction pathway[52–54] has allowed the normal-stress dependence of the reaction rate to be measured and accurately modeled using Evans–Polanyi (E–P) perturbation theory.[55,56] The goal of the work outlined in the following is to use E–P perturbation theory to calculate the activation volumes for the hydrostatic-pressure dependences of the rates of Diels–Alder cycloaddition reactions.

Evans–Polanyi perturbation theory

The Evans–Polanyi (E–P) analysis is based on the idea that the reaction rate depends on the equilibrium constant between the initial- and the transition state.[39,40] The equilibrium constant for the overall reaction K depends on the standard, molar Gibbs free energy change for the process, ΔG°, as:

$$\Delta G^\circ = -RT\ln K, \tag{1}$$

where R is the gas constant and T is the absolute temperature.[57] E–P perturbation theory proposes that a modified version of eqn (1) can be written for the rate constant k as $\Delta G^\circ = -RT\ln K$, where ΔG° is now the Gibbs free energy change between the transition-state and initial-state.

Depending on the reaction conditions, the Gibbs free energy G of a system can include perturbations described by some intensive variable, I (such as pressure or stress), by using the associated extensive conjugate variable, C, such that IdC equals the reversible work done on the system, so that $G = U - TS + IC$.[58] In the case of a hydrostatic pressure, P, the conjugate variable is $-V$.[59] Evans and Polanyi[39,40] also used their perturbation theory to derive the Nernst and Tafel equations in electrochemistry.[60] This approach is quite general and can be used for calculating the dependence of a chemical reaction rate on any perturbation as long as the corresponding conjugate variable is known. The conjugate variable, C, can itself depend on I,[61] as was alluded to by Evans and Polanyi,[39,40] so that the general equation for the standard Gibbs free energy change becomes:

$$\Delta G^\circ = \Delta U^\circ - T\Delta S^\circ + I\Delta C^\circ(I). \tag{2}$$

When the reaction rate is modified by a hydrostatic pressure, P, then k, the pressure-dependent rate constant is given by: $\left.\frac{\partial \ln k(P)}{\partial P}\right|_T = -\frac{\Delta V^\ddagger}{RT}$, and integrating gives: $k(P) = k_0 \exp\left(-\frac{P\Delta V^\ddagger}{RT}\right)$, where P is the hydrostatic pressure, T the absolute temperature, k_0 is the rate constant in the absence of an external pressure, and $\Delta V^\ddagger$ is an activation volume. Assuming that the pre-exponential factor does not depend strongly on pressure and writing the rate constant in its Arrhenius form gives $E_{act}(P) = E_{act} + P\Delta V^\ddagger$. This commonly known as the Bell equation.[62] This method is distinct from non-equilibrium thermodynamics[63] and the Evans–Polanyi theory specifically applies to systems in which perturbations, such as a pressure or stress, modify the rate of a transition from one state to another over an activation barrier. This gives a linear dependence of the activation energy on pressure when the activation volume is a constant, but high-order dependences occur when the volume itself varies with pressure. There are

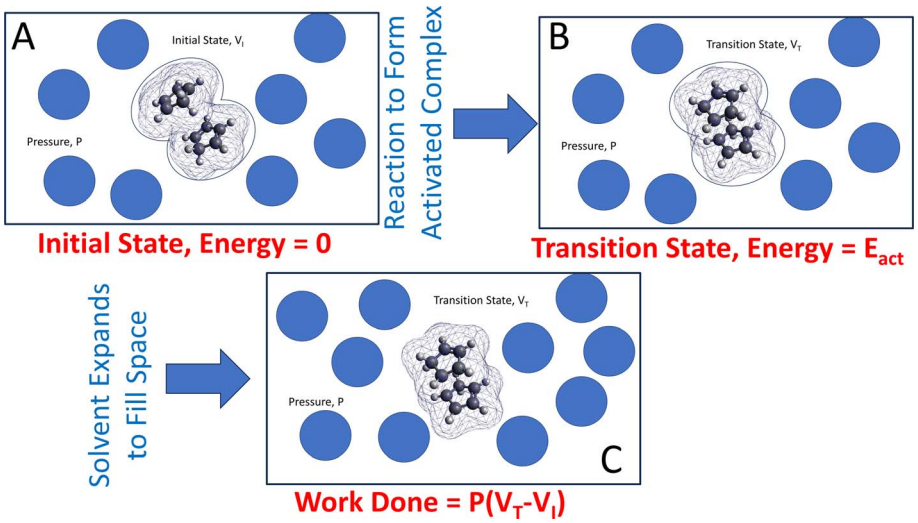

Fig. 1 Illustration of a calculation of the Gibbs free energy due to a hydrostatic pressure P for the Diels–Alder cycloaddition dicyclopentadiene showing (A) the initial-state structure shows the atom positions enclosed in a van der Waals' cage. (B) The transition-state structure with an energy E_{act}, which has a smaller volume than the initial-state structure. (C) The space created by the transformation is filled by the surrounding solvent where the contribution to the Gibbs free energy is $P(V_T - V_I)$.

several conceptual advantages to using such an Evans–Polanyi approach. As a consequence of Hess' law,[57] as for transition-state theory, the rate depends only on the properties of the initial- and transition states, and is independent of the pathway between them.[64,65]

Second, the theory directly yields a formula for the pressure-dependent rate constant, the value that is experimentally measured, and does not involve the reaction activation energy, although it can be obtained from the rate constant using the Arrhenius relation if the pre-exponential factor is known. Third, it can be used to simultaneously analyze the influence of multiple perturbations on the Gibbs free energy and therefore on the reaction rate. Finally, it is more efficient than having to calculate the full energy profile and thus is useful for high-throughput analyses.

The approach is illustrated in Fig. 1. A reacting ensemble (in this case, two cyclopentadiene molecules in a van der Waals' bound initial-state configuration) with volume V_I is surrounded by solvent molecules that collide with the reactants to exert a hydrostatic pressure P. During a reaction, the volume of the transition-state structure (the activated complex) changes to V_T. Note that this volume change was not induced by the hydrostatic pressure but is a change that takes place naturally as the reaction occurs. This contribution to the Gibbs free energy is $P(V_T - V_I)$ due to the surrounding solvent adjusting to maintain a constant pressure. This emphasizes the need to include the effect of the solvent on mechanochemical reactions that are carried out in solution. In the following analyses, the interaction is modeled using the polarizable continuum method (PCM).[66]

The same considerations apply in cases in which the reaction rate is modified by an AFM tip compressing or sliding on surfaces.[24,45,49–51] The reaction results in a change of tip position when it contacts the initial- and transition-state structures so it undergoes additional work $F(z_T - z_I)$, where F is the force and $(z_T - z_I)$ is the height difference between the transition- and initial state structures. Here, $(z_T - z_I)$ is known as the activation length.

However, as indicated by eqn (2), the perturbation can also change the value of conjugate variables, here the volumes, so that $V_T = V_T(P)$ and $V_I = V_I(P)$, so that the activation volume itself depends on pressure; $\Delta V^{\ddagger} = \Delta V^{\ddagger}(P)$. Methods for calculating this pressure dependence and for gauging its importance are also discussed.

Calculating linear-pressure-dependent reaction rates

Mechanochemical reaction rates are calculated using the perturbation method for transition-state theory developed by Evans and Polanyi[39,40] by modeling the surrounding solvent using the extreme-pressure polarizable continuum (XP-PCM) method.[46,47,66–68] This was not required for experiments carried out using an AFM tip *in vacuo*. An initial version of XP-PCM does not consider the distortion of the reacting ensemble inside the cavity and thus strictly measures an activation volume within the Bell approximation.

We first analyze the Diels–Alder cycloaddition of cyclopentadiene because the pressure-dependent kinetics have been independently measured by two different laboratories to provide pressure-dependent activation volumes,[41,42] which is then extended to analyzing other Diels–Alder reactions. The energy profiles were calculated using Gaussian 16 (ref. 69) to yield plots of the Gibbs free energy *versus* the intrinsic reaction coordinate (IRC). The Evans–Polanyi analysis only requires the effects on the initial- and transition-states to be calculated so that the influence of hydrostatic pressure and solvent on only these structures is calculated using the XP-PCM model.[46,47,66–68] This calculates the energies of the initial- and transition-state

structures embedded in a cavity of volume V_c that is constructed by enclosing them in van der Waals' spheres centered on the constituent atoms.[67] The cavity uses spheres of radii R_i centered on each nucleus of the atoms, where $R_i = fR_{vdW}$, and the R_{vdW} are the van der Waals' radii of each atom. Additional spheres are added to create a solvent-excluded surface cavity. The volume of the cavity is varied by adjusting the scaling factor f so that smaller values of f decrease the volume and increase the hydrostatic pressure.

The XP-PCM method calculates an electronic free energy, $G_{er}(P,\boldsymbol{R})$, where P is the pressure and $\boldsymbol{R}$ defines the nuclear positions. The cavity pressure is obtained from $P = -\dfrac{\partial G_{er}(P,\boldsymbol{R})}{\partial V_c}$ that also enables a so-called cavity free energy, $G_{cav}(P,\boldsymbol{R})$, to be calculated[66] to model the way in which the system interacts with a surrounding fluid. The method is described in greater detail elsewhere.[46,67] The total energy is given by $G_{tot}(P,\boldsymbol{R}) = G_{er}(P,\boldsymbol{R}) + G_{cav}(P,\boldsymbol{R})$. This method therefore differs from previous calculations of methyl thiolate mechanochemical reaction kinetics that were measured and modeled *in vacuo*.[45,55] Only the Gibbs free energies of the initial- and transition-state structures are required as a function of the cavity volume, V_c, obtained by varying the parameter f over the suggested range from 1.2 to 0.9.[46] As the cavity volume decreases, the energy of the system increases as the envelope interacts with the initial- or transition-state structures. The solvent is treated as a polarizable continuum with a uniform dielectric constant and the effect of solvent compressibility was taken into account using an η parameters, which was set to be 3. As such, the PCM methods is expected to work less well for polar reactants.

This Diels–Alder reaction has previously been analyzed by the XP-PCM method by performing energy calculations for structures throughout the whole reaction pathway,[67] while here it is implemented within the framework of an Evans–Polanyi analysis and thus only requires the values for the initial- and transition-states, $G^{I}_{er}(V_c)$ and $G^{T}_{er}(V_c)$, to be calculated as a function of the cavity volume, V_c. This is analogous to the results obtained by compressing a methyl thiolate species on a copper surface except that, in that case, the structures of the adsorbed methyl thiolate species were allowed to relax.[55] Since only the reactant molecules and the transition-state structures are analyzed, this allows energies to be calculated using small volume intervals allowing more precise fits to be made to plots of Gibbs free energy *versus* volume.

It has been found that the volume dependence of the Gibbs free energies can be reproduced quite well using a modification of the Murnaghan equation of state:

$$G_{er}(V_c) - G_{er}(V_c^0) = aV_c\left[\frac{1}{b-1}\left(\frac{V_c^0}{V_c}\right)^{b} + 1\right] + cV_c, \qquad (3)$$

where a, b and c are adjustable parameters, where a and c have units of pressure and b is unitless.[70] The Gibbs free energies are calculated as a function of cavity volume up to a reference value, V_C^0, when $f = 1.2$ to yield a Gibbs free energy, $G_{er}(V_c^0)$. Putting $x = \dfrac{V_c}{V_c^0}$, and using the constraint that $G_{er}(V_c) - G_{er}(V_c^0) = 0$ when $x = 1$ allows eqn (3) to be rewritten with the substitutions, $aV_c^0 = \alpha$, $cV_c^0 = \gamma$ and $\beta = b - 1$ to give:

$$G_{er}(x) - G_{er}(1) = \frac{\alpha}{\beta}x^{-\beta} + (\alpha + \gamma)x. \qquad (4)$$

The pressures are calculated from $P = -\dfrac{\partial G_{er}}{\partial V_c}$ to give P as a function of V_c using the fitting parameters, α, β, and γ for the initial- and transition-state structures to yield:

$$P = \frac{1}{V_c^0}\left[\alpha x^{-(\beta+1)} - (\alpha + \gamma)\right]. \qquad (5)$$

The pressure associated with each scaling factor f is then determined by averaging the pressure over all structures. This yields $G^{R}_{er}(\bar{P})$ and $G^{T}_{er}(\bar{P})$. $G_{tot}(\bar{P})$ for each structure is then computed by:

$$G_{tot}(\bar{P}) = G_{er}(\bar{P}) + G_{cav}[P], \qquad (6)$$

where $G_{cav}[P]$ is the cavitation energy for the molecular cavity and is described in greater detail elsewhere.[46,67] Eqn (6) yields the pressure dependence of the Gibbs free energy for a molecular species embedded in the solvent, and subsequently yields the activation volume, $\Delta V^{\ddagger} = -\dfrac{\partial(G^{T}_{tot} - G^{R}_{tot})}{\partial P}$. Note here that the initial-state structures used in the XP-PCM calculations are those of isolated reactant molecule, rather than the van der Waals' bound initial-state depicted in Fig. 1. That is, the initial-state energies and volumes represent the isolated reactant molecules in solution.

Evans–Polanyi theory indicates that a pressure-dependent rate constant $k(P)$ is given by: $\left.\dfrac{\partial \ln k}{\partial P}\right|_T = -\dfrac{V_T^0 - V_R^0}{RT} = -\dfrac{\Delta V^{\ddagger}}{RT}$. This equation can be integrated to give:

$$RT\ln\left(\frac{k(P)}{k_0}\right) = -\Delta V^{\ddagger}P, \qquad (7)$$

and can be directly compared with experiments.

Note that this analysis includes the effect of the environment, but not distortions of the initial- and transition-state structures during compression. This approach therefore allows the importance of various contributions to the mechanochemical reaction rates to be gauged, in particular the influence of distortions at higher pressures. The way in which they are calculated is discussed below.

Calculating second-order pressure-dependences

As noted above, the activation volume can itself depend on pressure. It has been suggested that molecular distortions are key to modifying the rates of mechanochemical reactions,[71,72] while the above analysis indicates that they do not to contribute the Bell-like, linear force or pressure dependences. However, they do contribute to second-order effects. In order to estimate

the extent to which they contribute to mechanochemical activity, here we outline a method of calculating the stress dependence using the force constants (Hessians) of the initial- and transition-states. Hessians have previously been used to calculate force-dependent molecular distortions,[73,74] but calculating stress-dependent distortions requires knowing the area over which the forces act. We note that, in the latest development of XP-PCM, geometry optimization under pressure is possible so that distortion of the reacting molecules could, in principle, be directly studied by XP-PCM.[75] However, the current implementation of XP-PCM geometry optimization only works well for small molecules. For larger systems, such as the Diels–Alder reactions studied here, there tends to be convergence problems in the geometry optimization, which prompts us to use this alternative approach to study molecular distortion.

Stress- (as opposed to force-) dependent distortions can be calculated from the values of the initial- and transition-state Hessians obtained from the quantum calculations by using the Stearn–Eyring approximation that relates the activation volume to the activation length.[76] The shape of the potential energy surface as a function of the position vectors of the atoms, $U(\boldsymbol{R})$, can be expanded up to second order about the turning points (the minimum (initial state) or a saddle point (transition state)). Since, by definition, their first derivatives are zero, the potential is:

$$U(\boldsymbol{R}) = U_0 + \frac{1}{2}\sum_k\sum_{\alpha,\beta}\left.\frac{\partial^2 U}{\partial d_{k\alpha}\partial d_{k\beta}}\right|_0 d_{k\alpha}d_{k\beta}, \quad (8)$$

where α and β correspond to Cartesian coordinates x, y and z, and $d_{k\beta}$ are the displacements of the kth atom along the α directions from their equilibrium positions, and $\left.\frac{\partial^2 U}{\partial d_{k\alpha}\partial d_{k\beta}}\right|_0 = k^k_{\alpha\beta}$ is the force constant (Hessian) matrix of the system. This can be written in matrix notation as $U = U_0 + \frac{1}{2}\boldsymbol{d}^{\mathrm{T}}\boldsymbol{k}\boldsymbol{d}$.

It is convenient to describe the potential energy using normal coordinates $\boldsymbol{Q}$ that involve the motion of all atoms of the reacting system. We introduce a $3N \times 3N$ matrix $\boldsymbol{L}$ that transforms the coordinates from $\boldsymbol{d}$ to another system $\boldsymbol{Q}$ as $\boldsymbol{Q} = \boldsymbol{L}^{-1}\boldsymbol{d}$ and $\boldsymbol{d} = \boldsymbol{L}\boldsymbol{Q}$,[77] so that eqn (8) becomes $U = U_0 + \frac{1}{2}\boldsymbol{Q}^{\mathrm{T}}\boldsymbol{L}^{\mathrm{T}}\boldsymbol{k}\boldsymbol{L}\boldsymbol{Q}$. Since the displacements are real and since $\boldsymbol{L}^{-1}(\boldsymbol{L}^{-1})^{\mathrm{T}} = \boldsymbol{I}$, where $\boldsymbol{I}$ is the identity matrix, then $\boldsymbol{L}^{\mathrm{T}}\boldsymbol{L} = \boldsymbol{I}$. For a non-singular matrix $\boldsymbol{L}$, then $\boldsymbol{L}^{\mathrm{T}} = \boldsymbol{L}^{-1}$, so that $\boldsymbol{L}$ is an orthogonal matrix. We now choose a particular $\boldsymbol{L}$ matrix such that it diagonalizes the force-constant (Hessian) so that $\boldsymbol{L}^{\mathrm{T}}\boldsymbol{k}\boldsymbol{L} = \boldsymbol{\Lambda}$, where $\boldsymbol{\Lambda}$ is a diagonal $3N \times 3N$ force-constant matrix with elements $\lambda_1, \lambda_2, \lambda_3, \ldots\lambda_{3N}$, and $k_{ii} = \lambda_i$ and $k_{ij} = 0$ for $i \neq j$. Multiplying this equation by $\boldsymbol{L}$ yields the following eigenvalue equation:

$$\boldsymbol{k}\boldsymbol{L} = \boldsymbol{L}\boldsymbol{\Lambda}, \quad (9)$$

so that $\boldsymbol{L}$ is an eigenfunction of $\boldsymbol{k}$ with eigenvalues λ_i, corresponding to the force constants for each normal coordinate of $\boldsymbol{Q}$, denoted by $\boldsymbol{Q}_i$. Each coordinate has its characteristic vibrational frequency, corresponding to a normal mode of the system.[34,78] The PES in eqn (8) is expanded up to second order as $U = U_0 + \frac{1}{2}\boldsymbol{Q}^{\mathrm{T}}\boldsymbol{\Lambda}\boldsymbol{Q}$, and, since $\boldsymbol{\Lambda}$ is a diagonalized Hessian, gives:

$$U = U_0 + \frac{1}{2}\sum_i \lambda_i \boldsymbol{Q}_i^2 \quad (10)$$

where $i = 1\ldots3N$, six of which are rotations and translations in homogeneous phase, which become tilts and hindered translations for adsorbed species. They can be used to calculate how a force $\boldsymbol{F}$ distorts the initial- or transition-state structures. The distortion depends on the direction of the force relative to each normal coordinate and the value of the associated force constant; smaller force constants will lead to larger distortions. In the case of a chemical reaction, the smallest force constants are likely to be those corresponding to the reaction pathway that connects the initial- and the transition-state structures, $\lambda_{\mathrm{r}}^{\mathrm{T}}$ and $\lambda_{\mathrm{r}}^{\mathrm{R}}$. The shapes of the potential-energy surfaces are $U_{\mathrm{T}}(\boldsymbol{Q}_{\mathrm{r}}^{\mathrm{T}}) \approx E_{\mathrm{act}} - \frac{1}{2}\lambda_{\mathrm{r}}^{\mathrm{T}}\boldsymbol{Q}_{\mathrm{r}}^{\mathrm{T}2}$ and $U_{\mathrm{R}}(\boldsymbol{Q}_{\mathrm{r}}^{\mathrm{R}}) \approx \frac{1}{2}\lambda_{\mathrm{r}}^{\mathrm{R}}\boldsymbol{Q}_{\mathrm{r}}^{\mathrm{R}2}$, where E_{act} is the reaction activation energy and the negative sign in this equation reflects the fact that the transition-state potential is a saddle point. To calculate the effect of a force on the structures, since $\boldsymbol{F} = \boldsymbol{\nabla}U$, then $\boldsymbol{Q}_{\mathrm{r}}^{\mathrm{R}} = -\frac{\boldsymbol{F}}{\lambda_{\mathrm{r}}^{\mathrm{R}}}$ and $\boldsymbol{Q}_{\mathrm{r}}^{\mathrm{T}} = \frac{\boldsymbol{F}}{\lambda_{\mathrm{r}}^{\mathrm{T}}}$. If the projected areas of the reactant molecules along directions parallel to $\boldsymbol{Q}_{\mathrm{r}}^{\mathrm{R}}$ and $\boldsymbol{Q}_{\mathrm{r}}^{\mathrm{T}}$ are A_{R} and A_{T}, then $\boldsymbol{Q}_{\mathrm{r}}^{\mathrm{R}} = -\frac{A_{\mathrm{R}}}{\lambda_{\mathrm{r}}^{\mathrm{R}}}P$ and $\boldsymbol{Q}_{\mathrm{r}}^{\mathrm{T}} = \frac{A_{\mathrm{T}}}{\lambda_{\mathrm{r}}^{\mathrm{T}}}P$, where P is the hydrostatic pressure. Substituting into the equations for the energy of the system gives a pressure-dependent energy change due to molecular distortion:

$$\Delta E(P) = -\frac{1}{2}\left[\frac{{A_{\mathrm{T}}}^2}{\lambda_{\mathrm{r}}^{\mathrm{T}}} + \frac{{A_{\mathrm{R}}}^2}{\lambda_{\mathrm{r}}^{\mathrm{R}}}\right]P^2. \quad (11)$$

Note that the positive initial-state and negative transition-state Hessians will generally lead to a reduction in activation volume at higher pressures. Evaluating this equation, however, requires knowing A_{T} and A_{R}, which can be determined from the activation volume calculated using XP-PCM when combined with an activation length obtained from the quantum calculations of the reaction as described in the following section. It should be noted that other, low-frequency modes of flexible functional groups attached to the reactants might also provide additional contributions to pressure-dependent changes to the activation volume.

Calculating values of A_{R} and A_{T}

Evans–Polanyi theory indicates that the activation length corresponds to a vector connecting the initial and transition states. Since the initial states for Diels–Alder reactions are more compliant than for the transition state,[46] it will have a greater influence on the energy barrier than the much sharper transition state. This occurs because of the weak van der Waals' interactions between the initial-state reactants in this biomolecular process compared to the transition-state structure,

which has shorter-range, bond-forming interactions. If we define the activation length relative to the initial state-location as $\Delta x^{\ddagger}$, then the Stearn–Eyring approximation gives $\Delta V^{\ddagger} = A_T \Delta x^{\ddagger}$,[76] so that we now need the correspond value of A_R. However, microscopic reversibility requires that the activation length for the reverse reaction is $-\Delta x^{\ddagger}$, which defines an activation length relative to the transition-state. This is equivalent to a force acting in the reverse direction and will have an activation volume of $-\Delta V^{\ddagger}$ so that the Stearn–Eyring approximation now gives $-\Delta V^{\ddagger} = -A_R \Delta x^{\ddagger}$, so that $A_T = A_R$, so that eqn (11) becomes: $\Delta E(P) = -\frac{1}{2}\left[\frac{1}{\lambda_r^T} + \frac{1}{\lambda_r^R}\right] A_C{}^2 P^2$, where now A_C is the area over which the stress acts and equals both A_R and A_T.

This is first applied to the cyclopentadiene dimerization reaction with a view to establishing whether the XP-PCM method can be implemented within the framework of the Evans–Polanyi approach to reproduce the experimental mechanochemical reaction kinetics and secondly, to show how effects due to molecular distortions can be obtained using parameters that are directly available from DFT calculations and to establish how important they are over the range of pressures that are routinely available in mechanochemical processes. The Diels–Alder cycloaddition of cyclopentadiene[41,42,46,48] was selected first because experimental results were obtained independently by two different groups, and the rates were also measured as function of pressure to allow the magnitude of second-order effects to be gauged.[41,42] The method was then applied to other Diels–Alder reactions, methyl acrylate and isoprene,[79] methyl acrylate and cyclopentadiene,[42] isoprene dimerization,[80] methyl vinyl ketone dimerization,[80] and isoprene and methyl vinyl ketone,[80] to further test the validity of the Evans–Polanyi approach and to gauge the relative importance of molecular distortion to the overall mechanochemical reactivity. Note that the results for polar reactants are likely to be less reliable that those for non-polar ones because of the limitations of the PCM method.

Results: hydrostatic-pressure induced Diels–Alder reactions: cyclopentadiene dimerization

We apply the Evans–Polanyi analysis to hydrostatic-pressure-modified mechanochemical reactions implemented using the XP-PCM method.[43,44] We illustrate the approach for the Diels–Alder dimerization of cyclopentadiene *via* the endo reaction pathway. A polynomial fit, $G_{tot}(P) - G_{tot}[f = 1.2] = a + bP + cP^2$ (see Fig. S2†) yields values of the parameters a, b, and c for the initial- and transition-states that are summarized in Table 1.

The resulting plots (see Fig. S2†) are quite linear indicating that, despite the reacting ensemble interacting with the surrounding solvent, the behavior is still Bell-like and the activation volume is pressure independent.

The experimental results are shown in Fig. 2 as a plot of $RT \ln\left(\frac{k(P)}{k_0}\right)$ *versus* P, where eqn (7) indicates that the slope corresponds to $-\Delta V^{\ddagger}(P)$; the positive slope here corresponds to a decrease in volume in going from the initial to the transition state, *i.e.*, a negative activation volume. Experiments were carried out independently by two groups.[41,42] In particular, the rates were measured by Walling[41] at several temperatures where all the data collapse onto a single plot when the temperature is taken into account (eqn (7)). The results are also in very good agreement with those obtained by Seguchi (♦).[42] The solid black line shows the Bell-like results obtained from the XP-PCM theory as described above, and is in good agreement with experiment and yields an activation volume of −36.9 Å^3 per molecule (−22.2 cm^3 mol^{-1}).

Table 1 Value of the best-fit parameters a, b, and c to a second-order polynomial for the initial- and transition-states for the pressure-dependent Diels–Alder dimerization of cyclopentadiene, where the energies are in J mol^{-1} and pressures are in J cm^{-3}

	Initial state	Endo transition state
a	−78947.468	−139769.230
b	94.009	165.803
c	0.0006	0.0011

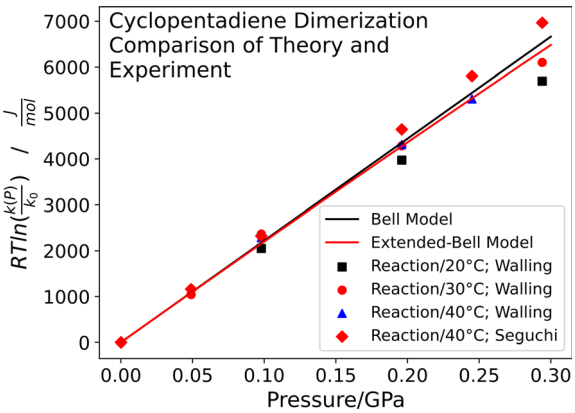

Fig. 2 Plot of $RT \ln\left(\frac{k(P)}{k_0}\right)$, corresponding to the stress-dependence change in reaction activation energy in J mol^{-1}, *versus* hydrostatic pressure in GPa, showing the experimental collected by Walling *et al.* (■, ● and ▲)[41] and by Seguchi *et al.* (♦).[42] The theoretical prediction (black solid line) without pressure-induced distortion of the reaction ensemble (the Bell approximation) and including distortion by using the force constants (solid red line).

In order to investigate the influence of compliant initial and transition-states, and thus to gauge the extent of an extended-Bell-type contribution to the mechanochemical activity of cyclopentadiene dimerization,[81] we compute the initial-state and transition-state force constants from Gaussian. We note that this could, in principle, have been estimated by allowing the structures of the reacting ensembles to relax for each compression step as was done for the normal-stress-induced decomposition of methyl thiolate species on copper.[55]

The activation volume obtained from the theoretical slope in Fig. 1 (−36.9 Å^3 per molecule) and the locations of the reactants in the initial and transition states, $\Delta x^{\ddagger} = 1.51$ Å per molecule

(see Fig. S8R†), gives $A_C = 24.43$ Å^2 per molecule. The Gaussian calculation yields force constants of the initial- and transition-state energy profiles of $k_R = \frac{1}{\lambda_R} = 8.43$ N m^{-1} and $k_T = \frac{1}{\lambda_T} = -148.95$ N m^{-1}. Note that the more compliant initial state will have a dominant influence on the P^2 dependence. The potential energy surface used to calculate the value of the activation length also shows the shape of the potential about the initial- and transition-states. Harmonic fits are shown in Fig. S8R,† and reproduce the shape of the potential over quite a large range and yield the above values of k_R and k_T, in good agreement with the values for the transition state calculated directly from Gaussian (see ESI Section†). Similarly good agreement was obtained for the other Diels–Alder reactions. The results are plotted as a red solid line in Fig. 2 and show very little difference from those without the distortion (black line), suggesting that, under the pressures exerted in normal laboratory experiments of ~0.3 GPa, the effect of molecular distortions is negligible.

Results: other hydrostatic-pressure induced Diels–Alder reactions

The XP-PCM analysis using the Evans–Polanyi method was applied to calculating the activation volumes for other Diels–Alder cycloaddition reactions, which tend to be relatively insensitive to pressure[82] and activation volumes measured for a Diels–Alder cycloaddition reactions in several different solvent yielded a standard variation of ~0.7 cm^3 mol^{-1}.[83] Note that the results, unlike the cyclopentadiene dimerization reaction, were from a single set of experiments so were not independently corroborated. The results are summarized in Table 2 and agree with experiment within a single standard deviation for non-polar reactants, cyclopentadiene and isoprene, as expected for the PCM method. As anticipated, the agreement for non-polar reactants is less good and tends to underestimate the value of the activation volume by ~10 cm^3 mol^{-1}, possibly due to short-range interactions between the solvent and the reactant causing the force exerted on the reactants to be larger than it would have been. This idea can be tested by including a coordination sphere of solvent molecules around the reaction ensemble and embedding that in a polarizable continuum to explore whether this might be a method of enhancing mechanochemical reactivity.

The effect of molecular distortion on the activation volumes was calculated from the values of the force constants, activation lengths and areas over which the pressure acts using the method described above. The plots of energy as a function of the displacement of the diene and dienophile for these reactions are summarized in the ESI Section (Fig. S8†). The force constants were calculated for the initial- and transition-states with harmonic fits to the initial-and transition-state potentials plotted in Fig. S8.† The parabolic fits to the data cover quite a wide range and the resulting values are in good agreement with the force constants from Gaussian and the results are shown in Table 3. The last column shows the relative change in activation volume under the influence of a pressure of 0.3 GPa, where the corresponding change for cyclopentadiene dimerization, where the results are plotted in Fig. 2, is ~5%. The results are within the errors limits of the measurements. However, since the change in activation volume scales as the square of the pressure, higher-pressure contacts such as in a ball mill will likely require second-order corrections. Note that the changes for the remainder of the reactions are of the order of a few percent.

Table 2 Summary of a comparison of the measured activation volumes with those calculated using the Evans–Polanyi method implemented using XP-PCM to calculate the interactions with the surrounding solvent for the following reactions for cyclopentadiene dimerization,[4,41] methyl acrylate and isoprene,[80] methyl acrylate and cyclopentadiene,[42] isoprene dimerization,[79] methyl vinyl ketone dimerization,[80] and isoprene and methyl vinyl ketone.[80] The activation volumes were generally measure by measuring the reaction rates as a function of hydrostatic pressure and then extrapolating to zero pressure. The uncertainty in the values of activation volume are taken to be 2.0 cm^3 mol^{-1} unless the error is specifically indicated in the reference. * indicates the lowest energy pathway from gas-phase calculations. CPD = cyclopentadiene, IP = isoprene, MA = methyl acrylate, MVK = methyl vinyl ketone

System	$\Delta V^{\ddagger}(0)_{calc}$ cm^3 mol^{-1}	$\Delta V^{\ddagger}_{expt}$ cm^3 mol^{-1}
CPD + CPD		
Endo	−22.2*	−23.7 ± 2.0
Exo	−21.4	
CPD + MA		
Endo	−21.6	−30.1 ± 2.0
Exo	−21.3*	
IP + IP		
Endo-1	−21.6	−24.3 ± 2.0
Endo-2	−22.6	
Exo-1	−21.5*	
Exo-2	−19.4	
IP + MA		
Endo-1	−23.5	−30.7 ± 2.0
Endo-2	−24.0	
Exo-1	−22.5*	
Exo-2	−21.9	
IP + MVK		
Endo-1	−24.8	−36.9 ± 2.0
Endo-2	−26.3	
Exo-1	−23.6*	
Exo-2	−22.9	
MVK + MVK		
Endo	−26.9*	−36.0 ± 2.0
Exo	−24.0	

Discussion

A perturbation method to transition-state theory first proposed by Evans and Polanyi has been applied to hydrostatic-pressure-modified Diels–Alder reactions. This general approach has previously been used to calculate pressure-dependent shear

Table 3 The effect of a hydrostatic pressure of 0.3 GPa on the activation volume using the force constant and the activation volume values shown in Table 2 from the activation lengths, $\Delta x^{\ddagger}$, to obtain a value of A_C, the area over which the stress acts, and the compliances of the initial and transition states to give the pressure-dependent change in activation volume given by eqn (11). The change in activation volume is shown in the last column. CPD = cyclopentadiene, IP = isoprene, MA = methyl acrylate, MVK = methyl vinyl ketone

System	$\Delta x^{\ddagger}$ nm	A_C nm^2	k_I N m^{-1}	k_T N m^{-1}	$\Delta\Delta V^{\ddagger}$ (0.3 GPa)$_{theory}$ cm^3 mol^{-1}	$\left\lvert\frac{\Delta\Delta V^{\ddagger}(0.3\ \text{GPa})}{\Delta V^{\ddagger}(0)}\right\rvert$
CPD + CPD						
Endo	0.151	0.244	8.43	−148.95	1.21	0.05
Exo	0.153	0.232	10.37	−140.51	0.87	0.04
CPD + MA						
Endo	0.141	0.254	9.83	−115.59	1.09	0.05
Exo	0.140	0.252	9.59	−114.74	1.10	0.05
IP + IP						
Endo-1	0.172	0.209	7.44	−170.15	1.01	0.05
Endo-2	0.182	0.206	5.87	−170.04	1.26	0.05
Exo-1	0.155	0.230	9.21	−169.50	0.98	0.05
Exo-2	0.167	0.193	6.16	−175.50	1.06	0.05
IP + MA						
Endo-1	0.147	0.266	8.07	−140.17	1.49	0.06
Endo-2	0.169	0.236	4.55	−143.39	2.14	0.09
Exo-1	0.193	0.193	3.13	−136.75	2.11	0.09
Exo-2	0.162	0.224	5.59	−144.10	1.56	0.07
IP + MVK						
Endo-1	0.143	0.288	7.86	−133.33	1.80	0.07
Endo-2	0.173	0.253	4.30	−137.60	2.60	0.10
Exo-1	0.155	0.252	5.33	−132.89	2.07	0.09
Exo-2	0.157	0.242	5.57	−141.29	1.83	0.08
MVK + MVK						
Endo	0.150	0.297	7.95	−136.43	1.89	0.07
Exo	0.141	0.283	12.80	−157.72	1.04	0.04

strengths of a sliding interface that yielded formulae that were in good agreement with those proposed on the basis of experiments.[56] The same approach was used to predict the normal-stress-induced rates of the mechanochemical decomposition of ethyl thiolate species adsorbed on a Cu(100) surface measured in vacuum that was also in excellent agreement with experiments carried out on a well-characterized in UHV.[55] Similar good agreement is found between experiment and theory for Diels–Alder cycloaddition reactions carried out in solution, where the interaction between the reactants and the solvent was modeled using the PCM method.

In a similar way that transition-state theory has been advantageous for understanding thermal reaction rates and mechanisms, the perturbation method of transition-state theory preserves those advantages and additionally provides conceptual insights into the way static stresses modify the rates of chemical reactions and gives a physical meaning to the activation volume parameter that describe the phenomena.

We note that the E–P method is quite general and can include the effect of several simultaneous perturbations. Consequently, it can straightforwardly be extended to analyzing processes that include both normal and shear stresses.[56] It could also investigate the combined effects of electric, magnetic or gravitational fields on mechanochemical reaction rates.

Like transition-state theory, the approach is fundamentally rooted in thermodynamics with all its associated advantages. Perhaps the most important is that the results depend only on the initial and final states of the system and is independent of the path taken between them.[49] This accelerates the calculation and this approach can be viewed as a high-throughput method, but this is not the primary benefit.

We find that an Evans–Polanyi analysis implemented by the XP-PCM method gives good agreement with experiment within the Bell approximation in which the initial- and transition-state structures are assumed to be rigid for non-polar reactants. However, the reactant and transition-state structures can distort under the influence of applied forces/stresses, resulting in quadratic force/stress dependences of the activation energy, sometimes known as the extended-Bell model.[81] This results in the activation volume/length depending on the stress/force as suggested in eqn (2). This causes the location of the transition-state structure to move closer to the reactants and the location of the reactants to move closer to the transition state,[82] known as the Hammond effect[11,64] by analogy to a similar effect found in organic chemistry.[83] It should be noted that mechanochemical reactions are still thermally driven and only require a reduction is energy barrier to result in significant increases in reaction rates. Because measurements of the effect of

hydrostatic pressure on reaction rates are made at pressures of 1 GPa or less,[43,44] the influence of molecular distortion was gauged using the force constants for various Diels–Alder reactions adapted to stress-induced reactions. This required a knowledge of the area over which the stress acts, which was calculated from the activation volume and the value of the activation length using the Stearn–Eyring relation.[76] This suggested that the influence of molecular distortion is not significant at a normal stress of ~0.3 GPa, warranting the use of the Bell approximation for analyzing these systems.

These results suggest that the polarizable-continuum methods works well and gives quantitative agreement between experiment and theory for reactions that involve non-polar, hydrocarbon reactants. Thus, the weak solvent-reactant interaction allows the continuum approximation to work well. In addition, the small pressure increments (see Fig. S2–S7†) allow precise values of the pressure to be calculated. However, the systematic difference of ~8 cm^3 mol^{-1} between experiment and theory (Table 2) implies that effect of the solvent is due to local, short-range interactions. This suggests that the XP-PCM method could be applied to polar reactants by including a first coordination sphere of solvent molecules surrounding the reacting ensemble embedded in a polarizable continuum.

Conclusions

This paper shows how the Evans–Polanyi perturbation method can be applied to analyzing the pressure-dependent Diels–Alder cycloaddition of cyclopentadiene, for which there are independent and corroborative experimental results, using the extreme-pressure polarizable continuum (XP-PCM) model. This was extended to a series of other Diels–Alder reactions in which the results were in good agreement with experiment for non-polar reactants, while the result for non-polar reactants were ~8 cm^3 mol^{-1} larger than the calculated results. This effect was proposed to be due to the reactants appearing to be larger due to interactions with the solvent.

The hydrostatic-pressure dependence is calculated just for the initial- and transition-state structures enclosed in a van der Waals' cocoon using XP-PCM model, where the reaction ensembles are not allowed to distort under the influence of the pressure. Note that only having to calculate the pressure dependence of the initial- and the transition-state structures allows the results to be obtained for a finer variation of cocoon volumes than would otherwise have been feasible. This allowed a full set of calculations to be rapidly carried out so that this approach is readily applicable to a wide range of pressure-modified mechanochemical reactions and will be useful for high-throughput calculations.

The effect of pressure-induced distortions on the initial- and transition-state structures could, in principle, have been computed by allowing them to relax during each compression cycle, but that would significantly lengthen the computation time. Instead, we used the force constants of the initial- and transition-state structures to estimate the energy change due to molecular distortions. This required knowledge of the area over which the pressures were exerted and was estimated using the Stearn–Eyring postulate from the calculated activation volume and activation length. The P^2 dependence calculated in this way showed that it has a negligible effect on the activation volume suggesting that molecular distortion does not contribute to the mechanochemical response under stresses that can be routinely obtained in the laboratory for this type of high-pressure experiment.

Data availability

The data supporting this article have been included as part of the ESI.†

Author contributions

All authors contributed equally to the paper.

Conflicts of interest

The authors declare no competing financial interest.

Acknowledgements

We gratefully acknowledge the Civil, Mechanical and Manufacturing Innovation (CMMI) Division of the National Science Foundation under grant number 2020525 for support of this work. This work was also supported by the French Agency for Ecological Transition (ADEME) through the IMOTEP project.

References

1 J. Sohma, *Prog. Polym. Sci.*, 1989, **14**, 451–596.
2 V. V. Boldyrev and K. Tkáčová, *J. Mater. Synth. Process.*, 2000, **8**, 121–132.
3 V. I. Levitas, *Phys. Rev. B: Condens. Matter Mater. Phys.*, 2004, **70**, 184118.
4 M. K. Beyer and H. Clausen-Schaumann, *Chem. Rev.*, 2005, **105**, 2921–2948.
5 Z. V. Todres, *Organic Mechanochemistry and its Practical Applications*, Taylor&Francis, Boca Raton, FL, 2006.
6 B. M. Rosen and V. Percec, *Nature*, 2007, **446**, 381–382.
7 S. A. Mitchenko, *Theor. Exp. Chem.*, 2007, **43**, 211–228.
8 S. L. James, C. J. Adams, C. Bolm, D. Braga, P. Collier, T. Friscic, F. Grepioni, K. D. M. Harris, G. Hyett, W. Jones, A. Krebs, J. Mack, L. Maini, A. G. Orpen, I. P. Parkin, W. C. Shearouse, J. W. Steed and D. C. Waddell, *Chem. Soc. Rev.*, 2012, **41**, 413–447.
9 S. L. Craig, *Nature*, 2012, **487**, 176–177.
10 J.-L. Do and T. Friščić, *ACS Cent. Sci.*, 2017, **3**(1), 13–19.
11 D. E. Makarov, *J. Chem. Phys.*, 2016, **144**, 030901.
12 H. J. Theophrastus, *Theophrastus's History of Stones : with an English Version, and Critical and Philosophical Notes, Including the Modern History of the Gems, &C., Described by that Author, and of Many Other of the Native Fossils*, London, 1774.
13 R. Planer, *Curr. Anthropol.*, 2018, **59**, 228.
14 C. Suryanarayana, *Prog. Mater. Sci.*, 2001, **46**, 1–184.

15 S. Kipp, V. Šepelák and K. D. Becker, *Chem. Unserer Zeit*, 2005, **39**, 384–392.
16 R. S. Varma, *Green Chem. Lett. Rev.*, 2007, **1**, 37–45.
17 C. R. Hickenboth, J. S. Moore, S. R. White, N. R. Sottos, J. Baudry and S. R. Wilson, *Nature*, 2007, **446**, 423–427.
18 J. Ribas-Arino, M. Shiga and D. Marx, *Angew. Chem., Int. Ed.*, 2009, **48**, 4190–4193.
19 S. M. Hick, C. Griebel, D. T. Restrepo, J. H. Truitt, E. J. Buker, C. Bylda and R. G. Blair, *Green Chem.*, 2010, **12**, 468–474.
20 J. Ribas-Arino and D. Marx, *Chem. Rev.*, 2012, **112**, 5412–5487.
21 R. Boulatov, *Nat. Chem.*, 2013, **5**, 84–86.
22 G. A. Bowmaker, *Chem. Commun.*, 2013, **49**, 334–348.
23 C. C. Piras, S. Fernández-Prieto and W. M. De Borggraeve, *Nanoscale Adv.*, 2019, **1**, 937–947.
24 N. N. Gosvami, J. A. Bares, F. Mangolini, A. R. Konicek, D. G. Yablon and R. W. Carpick, *Science*, 2015, **348**, 102–106.
25 J. Zhang and H. Spikes, *Tribol. Lett.*, 2016, **63**, 1–15.
26 R. P. Glovnea, A. K. Forrest, A. V. Olver and H. A. Spikes, *Tribol. Lett.*, 2003, **15**, 217–230.
27 E. Pollak and P. Talkner, *Chaos*, 2005, **15**, 026116.
28 H. Eyring, *J. Chem. Phys.*, 1935, **3**, 107–115.
29 G. Henkelman, B. P. Uberuaga and H. Jonsson, *J. Chem. Phys.*, 2000, **113**, 9901–9904.
30 G. Henkelman and H. Jónsson, *J. Chem. Phys.*, 2000, **113**, 9978–9985.
31 G. Henkelman, G. Jóhannesson and H. Jónsson, in *Theoretical Methods in Condensed Phase Chemistry*, ed. S. D. Schwartz, Springer Netherlands, Dordrecht, 2002, pp. 269–302.
32 D. Sheppard and G. Henkelman, *J. Comput. Chem.*, 2011, **32**, 1769–1771.
33 B. Peters, in *Reaction Rate Theory and Rare Events Simulations*, ed. B. Peters, Elsevier, Amsterdam, 2017, pp. 183–208.
34 W. H. Miller, N. C. Handy and J. E. Adams, *J. Chem. Phys.*, 1980, **72**, 99–112.
35 T. H. Lowry and K. S. Richardson, *Mechanism and Theory in Organic Chemistry*, Harper & Row, 1987.
36 R. Rana, R. Bavisotto, N. Hopper and W. T. Tysoe, *Tribol. Lett.*, 2021, **69**, 32.
37 G. Subramanian, N. Mathew and J. Leiding, *J. Chem. Phys.*, 2015, **143**, 134109.
38 W. Quapp and J. M. Bofill, *Theor. Chem. Acc.*, 2016, **135**, 113.
39 M. G. Evans and M. Polanyi, *Trans. Faraday Soc.*, 1935, **31**, 875–894.
40 M. G. Evans and M. Polanyi, *Trans. Faraday Soc.*, 1936, **32**, 1333–1360.
41 C. Walling and H. J. Schugar, *J. Am. Chem. Soc.*, 1963, **85**, 607–612.
42 K. Seguchi, A. Sera and K. Maruyama, *Bull. Chem. Soc. Jpn.*, 1974, **47**, 2242–2246.
43 T. Asano and W. J. Le Noble, *Chem. Rev.*, 1978, **78**, 407–489.
44 A. Drljaca, C. D. Hubbard, R. van Eldik, T. Asano, M. V. Basilevsky and W. J. le Noble, *Chem. Rev.*, 1998, **98**, 2167–2290.
45 A. Boscoboinik, D. Olson, H. Adams, N. Hopper and W. T. Tysoe, *Chem. Commun.*, 2020, **56**, 7730–7733.
46 B. Chen, R. Hoffmann and R. Cammi, *Angew. Chem., Int. Ed.*, 2017, **56**, 11126–11142.
47 T. Yang, R. Fukuda, R. Cammi and M. Ehara, *J. Phys. Chem. A*, 2017, **121**, 4363–4371.
48 S. K. Jha, K. Brown, G. Todde and G. Subramanian, *J. Chem. Phys.*, 2016, **145**, 074307.
49 R. Rana, G. Djuidje Kenmoe, F. Sidoroff, R. Bavisotto, N. Hopper and W. T. Tysoe, *J. Phys. Chem. C*, 2022, **126**, 11585–11593.
50 R. Rana, N. Hopper, F. Sidoroff and W. T. Tysoe, *Chem. Sci.*, 2022, **13**, 12651–12658.
51 J. R. Felts, A. J. Oyer, S. C. Hernández, K. E. Whitener Jr, J. T. Robinson, S. G. Walton and P. E. Sheehan, *Nat. Commun.*, 2015, **6**, 6467.
52 O. J. Furlong, B. P. Miller, P. Kotvis and W. T. Tysoe, *ACS Appl. Mater. Interfaces*, 2011, **3**, 795–800.
53 O. Furlong, B. Miller and W. T. Tysoe, *Wear*, 2012, **274–275**, 183–187.
54 H. Adams, B. P. Miller, P. V. Kotvis, O. J. Furlong, A. Martini and W. T. Tysoe, *Tribol. Lett.*, 2016, **62**, 1–9.
55 N. Hopper, F. Sidoroff, R. Rana, R. Bavisotto, J. Cayer-Barrioz, D. Mazuyer and W. T. Tysoe, *Phys. Chem. Chem. Phys.*, 2023, **25**, 15855–15861.
56 N. Hopper, F. Sidoroff, J. Cayer-Barrioz, D. Mazuyer and W. T. Tysoe, *Tribol. Lett.*, 2023, **71**, 121.
57 T. L. Hill, *An Introduction to Statistical Thermodynamics*, Dover Publications, 1986.
58 R. Hill, *J. Mech. Phys. Solids*, 1968, **16**, 229–242.
59 R. A. Alberty, *Pure Appl. Chem.*, 2001, **73**, 1349–1380.
60 J. O. M. Bockris, *Electrochemistry*, Butterworths, University Park Press, London, Baltimore, 1973.
61 J. Spooner and N. Weinberg, *Can. J. Chem.*, 2016, **95**, 149–161.
62 G. Bell, *Science*, 1978, **200**, 618–627.
63 I. Prigogine, *Introduction to Thermodynamics of Irreversible Processes*, Interscience Publishers, New York, 1968.
64 S. S. M. Konda, J. N. Brantley, B. T. Varghese, K. M. Wiggins, C. W. Bielawski and D. E. Makarov, *J. Am. Chem. Soc.*, 2013, **135**, 12722–12729.
65 S. M. Avdoshenko and D. E. Makarov, *J. Phys. Chem. B*, 2016, **120**, 1537–1545.
66 J. Tomasi, B. Mennucci and R. Cammi, *Chem. Rev.*, 2005, **105**, 2999–3094.
67 R. Cammi, *J. Comput. Chem.*, 2015, **36**, 2246–2259.
68 R. Cammi, in *Annual Reports in Computational Chemistry*, ed. D. A. Dixon, 2017, vol. 13, pp. 117–135.
69 M. J. Frisch, G. W. Trucks, H. B. Schlegel, G. E. Scuseria, M. A. Robb, J. R. Cheeseman, G. Scalmani, V. Barone, B. Mennucci, G. A. Petersson, H. Nakatsuji, M. Caricato, X. Li, H. P. Hratchian, A. F. Izmaylov, J. Bloino, G. Zheng, J. L. Sonnenberg, M. Hada, M. Ehara, K. Toyota, R. Fukuda, J. Hasegawa, M. Ishida, T. Nakajima, Y. Honda, O. Kitao, H. Nakai, T. Vreven, J. A. Montgomery Jr, J. E. Peralta, F. Ogliaro, M. J. Bearpark, J. Heyd, E. N. Brothers, K. N. Kudin, V. N. Staroverov, R. Kobayashi,

J. Normand, K. Raghavachari, A. P. Rendell, J. C. Burant, S. S. Iyengar, J. Tomasi, M. Cossi, N. Rega, N. J. Millam, M. Klene, J. E. Knox, J. B. Cross, V. Bakken, C. Adamo, J. Jaramillo, R. Gomperts, R. E. Stratmann, O. Yazyev, A. J. Austin, R. Cammi, C. Pomelli, J. W. Ochterski, R. L. Martin, K. Morokuma, V. G. Zakrzewski, G. A. Voth, P. Salvador, J. J. Dannenberg, S. Dapprich, A. D. Daniels, Ö. Farkas, J. B. Foresman, J. V. Ortiz, J. Cioslowski and D. J. Fox, *Gaussian 09, Revision B.01*, Gaussian Inc., Wallingford, 2010.

70 R. Cammi, B. Chen and M. Rahm, *J. Comput. Chem.*, 2018, **39**, 2243–2250.

71 A. Khajeh, X. He, J. Yeon, S. H. Kim and A. Martini, *Langmuir*, 2018, **34**, 5971–5977.

72 J. Yeon, X. He, A. Martini and S. H. Kim, *ACS Appl. Mater. Interfaces*, 2017, **9**, 3142–3148.

73 K. Brandhorst and J. Grunenberg, *Chem. Soc. Rev.*, 2008, **37**, 1558–1567.

74 T. Stauch and A. Dreuw, *J. Chem. Phys.*, 2015, **143**, 074118.

75 R. Cammi and B. Chen, *J. Chem. Phys.*, 2022, **157**, 114101.

76 A. E. Stearn and H. Eyring, *Chem. Rev.*, 1941, **29**, 509–523.

77 M. Born and K. Huang, *Dynamical Theory of Crystal Lattices*, Clarendon Press, Oxford, 2002.

78 E. B. Wilson, J. C. Decius and P. C. Cross, *Molecular Vibrations : the Theory of Infrared and Raman Vibrational Spectra*, McGraw-Hill, New York, 1955.

79 C. Walling and J. Peisach, *J. Am. Chem. Soc.*, 1958, **80**, 5819–5824.

80 C. Brun and G. Jenner, *Tetrahedron*, 1972, **28**, 3113–3121.

81 S. S. M. Konda, J. N. Brantley, C. W. Bielawski and D. E. Makarov, *J. Chem. Phys.*, 2011, **135**, 164103–164108.

82 W. Tysoe, *Tribol. Lett.*, 2017, **65**, 48.

83 G. S. Hammond, *J. Am. Chem. Soc.*, 1955, **77**, 334–338.